第34卷 第9期 焊 接 学 报 Vol. 34 No. 9
2013年9月 TRANSACTIONS OF THE CHINA WELDING INSTITUTION September 2013

铂金丝超声键合正交试验及焊点质量评价

莫德锋[1]， 杨力怡[1]， 张晶琳[2]， 吴家荣[2]， 刘大福[1]
(1. 中国科学院上海技术物理研究所 传感技术国家重点实验室，上海 200083;
2. 中国科学院上海技术物理研究所 红外成像材料和器件重点实验室，上海 200083)

摘 要: 采用正交试验法对直径为20 μm的铂金丝进行超声波键合试验，并通过三轴测量显微镜观察键合区域形貌和测量键合点根部高度. 结果表明，在研究的4个参数中，键合时间、搜索高度和超声功率的影响都较大，而键合力的影响较小. 通过正交试验法可以快速获得较优的键合参数，最佳工艺条件为: 键合力0.013 N，键合功率0.325 W(W为键合区宽度)，键合时间30 ms，搜索高度0.2 mm. 键合点质量可以通过测量键合点根部高度进行评价，当根部高度在4～10 μm之间时，引线拉力均在0.03 N以上. 而且，当键合区接近椭圆形，且当$W \approx 2D$(D为引线丝直径)时，引线拉力较高，当键合区形貌为矩形或有裂纹出现时，拉力则较小.

关键词: 铂金丝; 超声波键合; 质量评价
中图分类号: TG146.3+3 **文献标识码**: A **文章编号**: 0253－360X(2013)09－0039－04

莫德锋

0 序 言

引线键合工艺由于简单、成本低廉、适应性强等特点在封装连接过程中占据主导地位，目前所有封装管脚的90%以上都采用引线键合连接[1]. 其中超声波引线键合是其重要手段，超声波键合是在施加压力的同时，在被焊件之间产生超声频率的弹性振动，破坏被焊件之间界面上的氧化层，并产生热量，使两固态金属牢固键合. 用于引线键合的金属丝主要有金丝、硅铝丝和铂金丝等，其中铂金丝的热导率只有硅铝丝的1/3和金丝的1/4[2]. 对于低温封装器件，引线漏热往往占有很大比重，因此对于引线数量多、工作温度低的器件封装，铂金丝是比较理想的键合材料. 但铂金丝刚性大，键合相对困难，目前国内外对引线键合的研究主要集中在金丝和硅铝丝[3,4]，对铂金丝的研究较少.

一般认为影响超声引线键合质量的因素众多[5-8]，从键合参数看，与超声功率、键合力、键合时间和搜索高度等有关; 从被键合表面看，与被键合表面清洁度、材料性质、处理工艺等有关. 超声引线键合涉及到材料、力学、物理、化学、摩擦学等多学科领域，且键合点的面积往往很小、键合过程时间短而难以观测，在控制相同键合条件的情况下，焊点质量也会相差很大，从而影响产品成品率. 文中从实际生产出发，采用正交试验法对铂金丝引线键合过程中的工艺参数进行研究，并通过焊点形貌观察和压焊点位置高度测试评价引线键合质量.

收稿日期: 2012－06－29
基金项目: 国家重点基础研究发展计划(973计划)资助项目(2012CB619200); 上海技术物理研究所创新专项资助项目(Q-ZY-67)

1 试验方法

超声波键合设备为KS公司4523楔形焊机，采用深腔45°穿丝劈刀对20 μm铂金丝进行键合，基板材料为宝石电极板，镀层材料为2 μm厚度的Ni和1 μm厚度的Au，在键合前试验基板用酒精溶液清洗干净并用氮气吹干.

由于影响键合质量的参数众多，相互关系不明确，根据预试验和生产经验的结果，以键合力(F)、超声功率(P)、键合时间(t)和搜索高度(H)为考察因素，其中搜索高度为0时，表示劈刀紧压电极板表面，搜索高度大于0则表示劈刀与电极板有一定距离. 最终以键合引线拉力值为考核指标，并设计$L_9 3^4$正交试验表，每个因素分别选取3个水平，见表1. 在键合试验时，保持尾丝长度为0.2 mm，抛丝高度为0.5 mm，跨丝长度约为3 mm，劈刀安装高度一致，并保持第一焊点的参数设置与第二焊点一致.

为了减小试验误差，每种状态键合引线30根，

表 1 键合因素水平表

Table 1 Levels of bonding factors

水平	键合力 F/N	超声功率 P/W	键合时间 t/ms	搜索高度 H/mm
1	0.010	0.325	20	0
2	0.013	0.390	30	0.1
3	0.007	0.455	40	0.2

在完成一根引线键合后，用 OLYMPUS SMT－6 三轴测量显微镜观察键合区域形貌并测量两键合点根部高度，根部高度是劈刀下压后铂金丝变形最大的平坦区域的厚度，测量位置如图 1 箭头所示区域. 用拉力计读出拉力值(f)，记录两压焊点中引起引线断裂的焊点高度值. 引线拉力用 30 个点拉力均值表示，在键合过程中若出现键合脱粘或断丝，则计该点拉力值为 0.

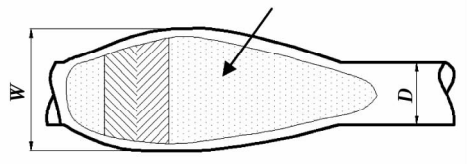

图 1 键合区域示意图

Fig. 1 Schematic diagram of bonding area

2 正交试验结果

正交试验结果如表 2 所示. 由于正交表具有搭配均匀的特性，各列上拉力的差异主要是由该列上不同水平引起的. K_1，K_2，K_3 分别为水平 1，水平 2，水平 3 数据的综合平均值. 各因素水平对拉力结果的影响可用该因素各水平间的极差 R 表示. 某因素的极差越大，就表明该因素对试验指标的影响也越大. 键合时间、搜索高度和超声功率的影响较大，而键合力的影响则较小. 较优工艺方案为(键合力、超声功率、键合时间、搜索高度，下角为水平)：$F_2P_1t_2H_3$，从表 2 中查得该条件下拉力均值为 0.051 N，为所有条件中的最高值，与正交分析结果相符. 一般认为，超声功率和时间对键合点的质量和外观影响显著，过小的功率会导致键合区域过窄、未形成有效键合或尾丝翘起，过大的功率导致根部断裂、键合塌陷或焊盘破裂[9,10]；而键合时间越长，引线吸收的能量越多，键合点的直径越大，界面强度增加而颈部强度降低，但是时间过长，会使键合点尺寸过大，超出焊盘边界并且导致空洞生成的概率增大[11].

为进一步了解其关系，以超声能量(键合功率与键合时间的乘积)与拉力均值作图，如图 2. 可以看出，各数值点基本呈统计学分布，尽管部分数值点有所偏离，主要原因是键合力和搜索高度不一致. 对于 20 μm 的铂金丝键合，在 9.75 mJ 输入能量附近，引线拉力出现一个峰值. 搜索高度会影响劈刀运动，当 $H=0$ 时，键合效果不佳，往往表现出键合点脱粘，需设置搜索高度在 0.1～0.2 mm 之间.

表 2 正交试验结果

Table 2 Results of orthogonal test

试验序号	水平				拉力均值
	F	P	t	H	f/N
1	1	1	1	1	0.024
2	1	2	2	2	0.041
3	1	3	3	3	0.010
4	2	1	2	3	0.051
5	2	2	3	1	0.015
6	2	3	1	2	0.034
7	3	1	3	2	0.024
8	3	2	1	3	0.041
9	3	3	2	1	0.011
K_1	0.025	0.033	0.033	0.017	
K_2	0.033	0.032	0.034	0.033	
K_3	0.025	0.019	0.016	0.034	
R	0.008	0.014	0.018	0.017	

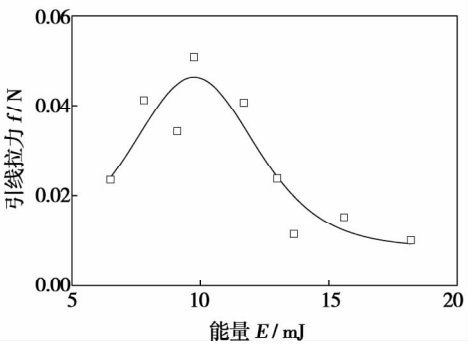

图 2 键合能量与引线拉力的关系

Fig. 2 Relationship between bonding energy and bonding strength

3 焊点形貌及质量评价

试验中也发现，即使键合条件一致，引线的拉力值也有较大波动，因此，在不破坏引线的前提下对引线质量进行评价在实际产品或工程项目中显得尤为重要.

观察焊点形貌是评价键合质量最简单的方法，通过显微镜观测焊点外形，可初步判断键合质量的

优劣. 但形貌观察比较定性,而且主观判断因素影响很大. 也有研究通过测量键合区域宽度来衡量[12],如图 1 中,引线丝直径用 D 表示,键合区宽度用 W 表示,一般认为,W 值应为 D 值的 1.2 ~ 3 倍. 但这种方法需反复寻找键合区域边界,操作不便,因此选择测量键合点根部高度进行评价.

图 3 显示了拉力值与键合点根部高度的关系,当键合点根部高度在 3 ~ 10 μm 时,随着键合点根部高度值的增大,拉力值增大,且大致呈线性关系. 但当键合点根部高度超过 10 μm 以后,拉力值并不继续增大,反而出现减小的趋势. 在观察过程中,没有发现键合点根部高度大于 12 μm 的焊点,可能原因是当键合点根部高度太大时,键合过程中塑性变形很小,很难获得较高的粘附力,易表现出铂金丝整体脱粘. 而当键合点根部高度小于 4 μm 时,键合点根部高度与拉力值无明显规律性,数值点随机分布,拉力值不稳定,而且拉力值小于 0.02 N 的点很多,影响键合的可靠性. 因此对于 20 μm 的铂金丝而言,键合点根部高度应保持在 4 ~ 10 μm 之间.

图 4 给出了几个典型的键合形貌,其对应的拉力值如图 3 所示. 可以看出,当焊接区形状接近椭圆形时能形成较好的强度,且当 $W \approx 2D$ 时,引线拉力较大. 当焊区形状接近矩形或者焊缝处有微裂纹出现时,则引线拉力较小,图 4 中 2 号和 3 号压点均出现了裂纹,因此拉力均小于 0.02 N.

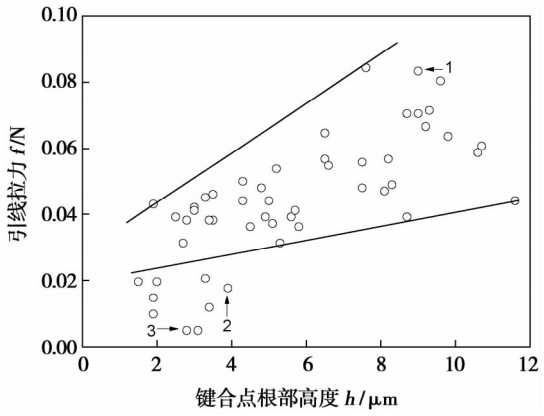

图 3　键合点根部高度与引线拉力的关系

Fig. 3　Relationship between height of bond heel and bonding strength

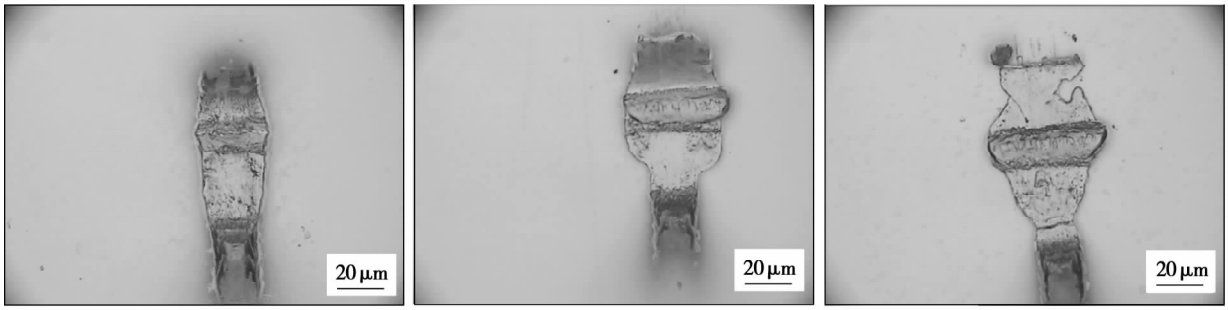

(a) 1号压点 $F_2P_1t_2H_3$　(b) 2号压点 $F_2P_2t_3H_1$　(c) 3号压点 $F_3P_3t_2H_1$

图 4　键合点形貌

Fig. 4　Microstructure of bonding areas

4　结　　论

(1) 在超声键合参数中,键合时间、搜索高度和超声功率的影响都较大,而键合力的影响则较小,最佳工艺条件为: 键合力 0.013 N,键合功率 0.325 W,键合时间 30 ms,搜索高度 0.2 mm.

(2) 引线拉力在适当能量输入条件下存在峰值,对于 20 μm 的铂金丝键合而言,当输入能量约为 9.75 mJ 时,引线拉力最大.

(3) 键合点质量可以通过测量键合点根部高度进行评价,当键合点根部高度在 4 ~ 10 μm 之间,引线拉力在 0.03 N 以上. 此外,当键合区接近椭圆形,且当 $W \approx 2D$ 时,引线拉力较大.

参考文献:

[1] 何　田. 引线键合技术的现状和发展趋势 [J]. 电子工业专用设备, 2004, 117(10): 12 - 14.
He Tian. Situation and development trend of equipment for wire bonding [J]. Electronic Products Marufacturing, 2004, 117(10): 12 - 14.

[2] 查尔斯 A. 哈珀编. 电子封装材料与工艺 [M]. 沈卓身, 贾松良, 译. 北京: 化学工业出版社, 2006.

[3] 旷仁雄, 谢　飞. 25 μm Au 丝引线键合正交试验研究 [J]. 半导体技术, 2010, 35(4): 369 - 372.
Kuang Renxiong, Xie Fei. Research of orthogonal test on 25 μm

gold wire bonding [J]. Semiconductor Technology, 2010, 35(4): 369 - 372.

[4] Ramminger S, Seliger N, Wachutka G. Reliability model for Al wire bonds subjected to heel crack failures [J]. Microelectronics Reliability, 2000, 40(9): 1521 - 1525.

[5] 宗 飞, 黄美权, 张汉民, 等. 引线键合中第一点勾线力的影响因素 [J], 电子与封装, 2011, 11(4): 12 - 16.
Zong Fei, Huang Meiquan, Zhang Hanmin, *et al*. Affecting factors of wire pull force in wire bonding [J]. Electronics & Packaging, 2011, 11(4): 12 - 16.

[6] 胡 蓉, 徐榕青, 李 悦. 微波电路引线键合质量的影响因素分析 [J], 电子工艺技术, 2009, 30(2): 92 - 95.
Hu Rong, Xu Rongqing, Li Yue. Effect factors analysis of wire bonding quality on microwave circuit [J]. Electronics Process Technology, 2009, 30(2): 92 - 95.

[7] 隆志力, 韩 雷, 吴运新, 等. 不同温度对热超声键合工艺连接强度的影响 [J], 焊接学报, 2005, 26(8): 23 - 26.
Long Zhili, Han Lei, Wu Yunxing, *et al*. Effect of different temperature on strength of thermosonic bonding [J]. Transactions of the China Welding Institution, 2005, 26(8): 23 - 26.

[8] 姜 威, 常保华, 都 东, 等. 引线键合中材料参数对硅基板应力状态的影响 [J], 焊接学报, 2012, 33(3): 13 - 16.
Jiang Wei, Chang Baohua, Du Dong, *et al*. Influence of wire materials and coating thickness on stress conditions in silicon substrate during copper thermosonic wire bonding [J]. Transactions of the China Welding Institution, 2012, 33(3): 13 - 16.

[9] 王福亮, 韩 雷, 钟 掘. 超声功率对引线键合强度的影响 [J]. 机械工程学报, 2007, 43(3): 107 - 111.
Wang Fuliang, Han Lei, Zhong Jue. Effect of ultrasonic power on the wire bonding strength [J]. Journal of Mechanical Engineering, 2007, 43(3): 107 - 111.

[10] Insu J, Qwanho C, Joonki H, *et al*. The effect of ultrasonic power on bonding pad and IMD layers in ultrasonic wire bonding [J]. Advances in Electronic Materials and Packaging, 2001, 9(01EX506): 19 - 22.

[11] 王福亮, 李军辉, 韩 雷, 等. 键合时间对粗铝丝超声引线键合强度的影响 [J]. 焊接学报, 2006, 27(5:): 47 - 51.
Wang Fuliang, Li Junhui, Han Lei, *et al*. Effect of bonding time on thick aluminum wire wedge bonding strengh [J]. Transactions of the China Welding Institution, 2006, 27(5): 47 - 51.

[12] 吕 磊. 引线键合工艺介绍及质量检验 [J]. 电子工业专用设备, 2008, 158(3): 53 - 59.
Lü Lei. The process introduction and quality inspection of wire bonding [J]. Equipment for Electronic Products Marufacturing, 2008, 158(3): 53 - 59.

作者简介: 莫德锋,男,1982 年生,博士. 主要从事封装结构设计与可靠性研究. 发表论文 20 多篇. Email: modefeng@163.com

通讯作者: 刘大福,男,博士,研究员. Email: sitp@163.com

tion in the heat-affected zone (HAZ) was simulated. The stress intensity factor at the cracking tip was calculated with SCC model, and the relationship between the stress intensity factor and cracking rate from the SCC propagation experiments was used to obtain the propagating rate of the crack. Consequently, the life of core shroud was predicted. This study solved the life prediction of important structures in nuclear reactor due to SCC failure, and also provided an useful method for life prediction of other important engineering structures.

Key words: core shroud; welded joint; stress corrosion cracking; finite element method; life prediction

Orthogonal test and quality evaluation of platinum wire ultrasonic bonding MO Defeng[1], YANG Liyi[1], ZHANG Jinglin[2], WU Jiarong[2], LIU Dafu[1] (1. State Key Laboratory of Transducer Technology, Shanghai Institute of Technical Physics, Chinese Academy of Sciences, Shanghai 200083, China; 2. Key Laboratory of Infrared Imaging Materials and Devices, Shanghai Institute of Technical Physics, Chinese Academy of Sciences, Shanghai 200083, China). pp 39 - 42

Abstract: Orthogonal test was applied to investigate the ultrasonic bonding of platinum wire with a diameter of 20 μm. The microstructure of bonded area was observed and the height of bonded heel was measured with three-axis measuring microscope. The results indicate that the influence of bonding time, search height and ultrasonic power on the platinum wire tensile force was very notable, while the effect of bonding force was relatively small. The optimized bonding parameters with high efficiency could be obtained through orthogonal test. The optimum conditions are listed as follows: the bonding force was 0.013 N, the bonding power was 0.325 W, the bonding time was 30 ms, and the search height was 0.2 mm. The bonding quality could be evaluated by measuring the height of bonded heel. The tensile force of the bonded wire exceeded 0.03 N when the bonded heel was 4 ~ 10 μm. Meanwhile, it was likely to acquire high bonding quality when the welded area was in elliptical shape and the W was equal to approximately 2D. Tensile force was low when the welded area was in rectangular shape or micro cracks appeared.

Key words: platinum wire; ultrasonic bonding; quality evaluation

Decoupling control analysis of aluminum alloy pulse MIG welding process based on dynamic fuzzy neural networks HUANG Jiankang[1], ZHANG Gang[2], FAN Ding[1], SHI Yu[2] (1. State Key Laboratory of Gansu Advanced Non-Ferrous Metal Materials, Lanzhou University of Technology, Lanzhou 730050, China; 2. Key Laboratory of Non-Ferrous Metal Alloys, The Ministry of Education, Lanzhou University of Technology, Lanzhou 730050, China). pp 43 - 47

Abstract: Considering the strong coupling of parameters, unstable and other key issues during aluminum alloy pulse MIG welding process, D-FNN structure and learning algorithm were introduced. The decoupling controllers were designed based on D-FNN. The dynamic decoupling control simulation of aluminum alloy pulse MIG welding multiple-input multiple-output (MIMO) process, setting the duty cycle of pulse current and wire feeding speed as inputs but wire extension and weld width as outputs, was investigated with synchronization, asynchronous and adding interference pulse. The simulation results indicate that D-FNN controller could real-time evolve rules, dynamically adjust the learning factors, completely decouple the MIMO process and meet the real-time control requirements of welding process. In addition, its fast response speed and good robustness provided a new real-time decoupling control method for stabilizing the aluminum alloy pulsed MIG welding process.

Key words: aluminum alloy pulse MIG welding; dynamic fuzzy neural networks; decoupling control; system simulation

Microstructure comparison of resistance butt welding and cold-pressure welding of zinc alloy wire ZHEN Liling, LIU Hongwei, FAN Jianxun, MING Zhu (Ningbo Branch of China Academy of Ordnance Science, Ningbo 315103, China). pp 48 - 50

Abstract: The fracture morphology of butt-welded joint with over mode was observed with metallographic microscope and scanning electron microscope (SEM) to enhance the overmoded rate of butt-welded joint of zinc alloy wire. The results show that the tension fracture of zinc alloy wire joint made by cold-pressure welding was ductile fracture of hardened material. The annealing should be performed ahead of the drawing process. After drawing the cold-pressure welded joint, the original bonding area widened and the separation of the streamline layers in bonded area became larger, and this was beneficial for releasing the stress concentration. The obvious grain growth with recrystallization occurred in resistance butt welded joint of zinc alloy wire. The generation of recrystallized grains was favorable for releasing the internal stress within the joint, which improved the plastic deformation capability of the joint and ensured the high overmoded rate of the resistance butt welded joint.

Key words: zinc alloy wire; drawing deformation; resistance welding; cold-pressure welding; recrystallization

HHT analysis of acoustic signal characteristics caused by defocusing amount fluctuation on laser strengthened mould surface LIU Lijun[1,2], JIANG Yaqing[2], DI Tienan[1], LI Jiqiang[2], JIA Zhixin[2], YANG Wenhao[3] (1. School of Materials Science and Engineering, Harbin University of Science and Technology, Harbin 150080, China; 2. Ningbo Institute of Technology, Zhejiang University, Ningbo 315100, China; 3. Ningbo Donghao Die-casting Co., Ltd., Ningbo 315113, China). pp 51 - 54

Abstract: During laser strengthening mould surface, the fluctuation of defocusing amount was caused by clamping and teaching errors, which greatly influenced the quality of laser strengthened mould surface. Thus, Hilbert-Huang Transform (HHT) analysis of acoustic signal characteristics caused by the fluctuation of defocusing amount on laser strengthened mould surface was put forward. According to the acoustic signal characteristics of laser strengthened mould surface, the HHT analysis steps were proposed. The mould life was improved over 20% when the mould surface was strengthened by the HHT analysis system. The experimental results provide a method for further re-